Electronic structure of nanopolycrystalline pulsed laser deposited LaB6 films and single crystals: the boron perspective

Liu, Lijia; Yiu, Y.M.; Sham, T.K.; Yang, Dongfang; Zuin, Lucia

Publisher's version / Version de l'éditeur:
https://doi.org/10.1063/1.3284935
Journal of Applied Physics, 107, 4, pp. 043703-1-043703-6, 2010

Electronic structure of LaB_6 single crystal and Pulsed Laser Deposited (PDL) films: The boron perspective

Lijia Liu, Y. M. Yiu and T.K. Sham
Department of Chemistry, University of Western Ontario
London ON, Canada N6A 5B7

Dongfang Yang
Industrial Materials Institute,
National Research Council Canada
London, ON Canada N6G 4X8

Lucia Zuin
Canadian Light Source, University of Saskatchewan
Saskatoon, SK S7N 0X4

Abstract

We report an investigation of the electronic structure of LaB_6 single crystal and Pulsed Laser Deposited (PLD) film with X-ray Absorption Near Edge Structures (XANES) spectroscopy at the B K-edge. The experimental results are compared with theoretical calculations using Density Functional Theory (DFT), the WIEN code, and real space multiple scattering, the FEEF8 code. It is found that (i) the B K-edge XANES for the single crystal specimens exhibit well defined spectral features corresponding to the theoretical partial densities of states of B p character and the threshold energy is relatively low and free electron like, revealing its metallic character, (ii) The LaB_6 PLD film is of high quality and also metallic albeit it is a polycrystalline phase of nanocrystallites, (iii) the surface of both single crystal and PLD film contains oxygen, especially the latter, which has a large interface area in its grain boundary. The implications of these observations are discussed.

I. Introduction

Lanthanium hexaboride, LaB_6, is a bright purple looking material with very unusual properties. For example, it is a refractory ceramic yet metallic and even superconducting at very low temperature [1]. It has a low work function and has therefore been exploited as electron emitting cathode or coating material for thermionic electron emitting cathode to increase its electron emission ability and to reduce its operation temperatures in, for example, electron microscopy applications. The relatively low work function yields higher current at low cathode temperature, resulting in greater brightness and longer cathode life. LaB_6 is also widely used as a standard material for instrument calibration [2] in X-ray powder diffraction for Rietveld analysis [3]. LaB_6 based materials are also found to exhibit weak magnetism [4].

Despite the above-mentioned properties and applications, the electronic structure of LaB_6 is still not fully understood [5-7]. This is especially the case when LaB_6 is fabricated in unusual dimensions such as thin films and nanostructures to increases emissivity. In this work, we report an investigation of the electronic structure of Pulsed Laser Deposited (PLD) LaB_6 film and LaB_6 (111) and (110) single crystal rods using X-ray Absorption Near Edge Structures (XANES) at the B K-edge. Theoretical calculation using Density Functional Theory (DFT) [8,9] with the Wien code [10], and real space multiple scattering theory with the FEFF8 code [11] have also been carried out to compare with the experimental data and to simulate model XANES.

XANES refers to the spectral features of the X-ray absorption coefficient above an absorption edge of an atom of interest in a chemical environment. In the vicinity of the threshold, it probes the unoccupied electronic states above the Fermi level with electronic dipole transitions. Thus B K-edge (1s) XANES provides information about the electron densities of states of boron with p character above the Fermi level. Since the energy of B K-edge is in the soft X-ray region (e.g. the attenuation length below and above the B K-edge at ~ 188 eV for LaB_6 is ~ 0.5 and ~0.05μm, respectively)[12], XANES measurements are often conducted in total electron yield and fluorescence yield for surface and bulk sensitivity, respectively [13,14]. XANES at these energies is sensitive to both the surface and the bulk of the specimen depending on the method of measurement; it can also provide chemical information along the sampling depth using different yield detection modes.

Although, there have been a couple of reports on the B K-edge of LaB_6, high resolution data and detailed interpretation are still lacking [5,6]. This work shows that PLD LaB_6 films are polycrystalline with nanocrystallites and that the experimental B K-edge XANES are in good agreement with DFT theory, probing the density of states within the single particle approximation.

II Experimental

LaB_6 coatings are usually deposited by magnetron sputtering; however, Ar implantation within the deposited film during sputtering could decrease their quality [15]. Higher quality films can be obtained by the pulsed laser deposition technique as the deposition can be performed under high vacuum. In this work, LaB_6 thin film was prepared by PLD from a LaB_6 target (stoichiometric, 99.95%) using an advanced deposition chamber (PVD Inc., PLD-3000) described in detail elsewhere [16]. The laser used was a KrF excimer with on target energy densities of ~ 5 J cm^{-2} (pulse duration 25 ns), and a repetition rate of 50 Hz. The ablation was carried out in vacuum with a pressure of 1.6 X 10^{-6} torr and a substrate temperature of 300 °C. A p-type 3" diameter Si(100) wafer (10-30 Ohm.cm) was used as the substrate; and was cleaned by a 5% HF solution according to the procedure described previously [16]. Deposition time was about 20 minutes. Single crystal LaB_6 (111) and (110) were obtained commercially (Applied Physics Technology) as 1mm x 5 mm rods. They exhibit sharp LEED (Low Energy Electron Diffraction) patterns.

The cross-sectional image of the LaB_6 film was taken by a Leo 440 field-emission scanning electron microscope (FE-SEM) and is shown in Figure 1. The thickness of the LaB_6 film, as determined from FE-SEM, is ~ 50 nm. FE-SEM revealed a textured LaB_6 film consisting of very fine grains with grain size less than 20 nm, presumably due to embedded crystalline LaB_6 nanostructures.

The film was also examined by X-ray diffraction (XRD, Philips, X-Pert MRD) in the θ_0-2θ thin film configuration using monochromatized Cu K_α X-rays, where θ_0 was fixed at a value of 0.5°. The diffraction pattern of the LaB_6 film shown in Figure 2 exhibits a diffuse-scattering curve with a broad band centered at 2θ of about 25°. Besides the broad band, several small peaks locating at 2θ of 21.4, 30.4 and 37.4 appear. These peaks correspond to the diffractions from (100), (110) and (111) planes of cubic LaB_6 (ICDD 34-0427) crystal, respectively. XRD results

clearly indicate that the PLD LaB_6 film consists of a uniform polycrystalline phase embedded with nanocrystallites.

The surface composition of the film and the singles crystals were check with XPS, using a Krotos Axis Ultra spectrometer at Surface Science Western. The XPS results clearly reveal a Fermi level in all the samples and the B and La core level before and after Ar ion sputtering clearly reveal the presence of surface oxide.

XANES measurements were carried out on the Variable Line Space Plane Grating Monochromator (VLS-PGM) Beamline of the Canadian Light Source [17]. This beamline provides high flux (> 10^{12} photon/sec) and high resolution ($E/\Delta E$ >10,000) photons in the energy range of 5 - 250 eV with three gratings. B K-edge measurements were conducted in both total electron yield (TEY), recoded as specimen current, and total fluorescence yield (FLY), recorded with a channel plate detector. No sputtering was used to preserve the integrity of the thin film. As noted above, TEY and FLY will be relatively surface and bulk sensitive, respectively. Since the thickness of the PLD film is only 50 nm, there will not be any significant self-absorption (thickness effect) in the FLY. The LaB_6 single crystals are mounted at a photon incident angle of ~ 45 ^{0} with respect to the crystal surface and there is no noticeable angle dependence in the spectral features due to the high symmetry of the B_6 octahedron unit in the cubic structure.

III. Theoretical calculation

LaB_6 crystal has a cubic structure of Pm3m with La occupying the 1a position of (000) and B at the 6f position of (1/2, 1/2, u) where u = 0.207. The unit cell dimension is a = 4.1566 Δ. The theoretical XANES spectra of LaB_6 have been calculated using two methods self consistently: (1) Density Functional Theory (DFT) [8] and Generalized Gradient Approximation (GGA) [9] using the WIEN code [10] and (2) Real Space Multiple Scattering (RSMS) using the FEFF8 program. [11]

The first method is the full potential augmented plane wave method used in the numerical calculation employing WIEN code. Crystals are described by unit cell with atoms occupying the symmetric atomic sites and interstitial area in between. The atomic sites are represented by spheres of bases, which are generated by a linear combination of radial wave functions and non-overlapping spherical harmonics. The interstitial regions are expressed by a

set of plane waves. The set of plane waves has been extended to 10000 number of plane waves in the present work. The boundary condition between the atomic sites and the interstitial area satisfies the Dirichlet condition. Scalar relativistic density function was used with GGA correction. Self-consistent minimization of energy was achieved with 1000 k points. In this numerical calculation, the tetrahedron method [18] for the k space integration was used. The theoretical XANES spectra were then calculated using the electrical dipole transition convoluted by instrumental Gaussian and core-hole lifetime Lorentzian broadenings [19].

In the second method, numerical calculation of XANES has been performed using the computer code FEFF8 self-consistently [11]. The program FEFF8 calculates clusters using an ab-initio self-consistent real space multiple scattering method. The calculations are based on relativistic Green's function formalism for all electrons. Clusters of 199 atoms of LaB_6 have been chosen for the FEFF8 calculation. Similar size of cluster were used for other simulations

IV Results and Discussion

Figures 3a, 3b and 3c shows the B K-edge XANES of LaB_6 (111), LaB_6 (110) and PLD LaB_6 film on Si(100), respectively, recorded in both TEY and FLY. Let us first look at the XANES for the single crystal specimens. We see from Figs. 3a and 3b that both exhibit similar spectral pattern with several sharp and well defined resonances above the threshold. Our data clearly reveal high resolution features not observed previously [5,6]. The main difference between TEY and FLY is the relative intensity of the peaks especially a sharp peak at 194.0 eV (calibrated to the same position as reported in ref. 5), which is most intense in the TEY and considerable weaker in the FLY. This speak has been observed before and was attributed to surface B-O bond of π^* character [5,6,18]. We will return to this peak below.

Fig. 3c shows that at first glance, the TEY and FLY XANES for the PLD LaB_6 film differs from those of single crystal samples markedly. Several features are noted. First, aside from the boron surface oxide peak at 194.0 eV, which is now the most dominant feature, all resonances are broadened. Second, the TEY shows that the sharp and well-defined features observed at first 5 eV above the threshold of XANES of the LaB_6 crystals are no longer present, instead, a broad and blue-shifted shoulder is observed; furthermore, the sharp features above the sharp peak (194.0 eV) in the XANES of the crystal samples are now replaced by a broad

resonance at ~202 eV. Finally, in the FLY, all the features seen in the crystals sample are observed albeit broadened, except for the feature at 191.73 eV which remains relatively sharp.

As noted above, the binding energy of B K-edge (B 1s threshold) falls on the soft X-ray energy range where the photon is attenuated very rapidly as it propagates into the sample. Thus for the single crystal samples, we have a total absorption situation; i.e. that all the incident photons are absorbed and FLY will suffer some thickness effect (self-absorption - the fluorescence X-ray was reabsorbed by the solid) whereas the PLD film is sufficiently thin so that the thickness effect is not significant. Thickness effect results in the broadening of the resonances especially for those with high absorption cross-sections as we can see from Figs. 3a and 3b.

We now concentrate on the XANES of the PLD film. In order to facilitate the interpretation of the data, we have removed the surface oxide contribution by subtracting the TEY signal after proper scaling from that of the FLY XANES of the PLD film and from the TEY XANES of the single crystal. This procedure is justified since the TEY of the PLD LaB_6 film is most representative of the surface/grain boundary oxide signal. The result of this analysis is shown in Fig. 4a and 4b for the XANES of the PLD film and the single crystal with B-O contribution minimized, respectively. We can now attribute the B K-edge XANES for the PLD film to a dominantly polycrystalline phase of LaB_6 with nano crystals of LaB_6 and a large surface/grain boundary area. This interpretation is based on the broadening of all the features and that the sharp features at 191.73 eV remains, this feature is associated with nanocrystals embedded in the film. This interpretation is consistent with the SEM (Fig. 1) and XRD (Fig. 2) results.

The experimental XANES for the single crystal LaB_6 can be compared with DFT calculation. Fig. 5 shows the partial densities of states (p-DOS) of B and La for the cubic LaB_6 crystal. Several features are apparent. First LaB_6 is metallic as can be seen at the continuing p-DOS of both B and La character across the Fermi level; this is confirmed by the appearance of a Fermi edge in the XPS. Second, the B p-DOS of p character exhibits three peak features within the first 5 eV above the Fermi level and a broader feature from 5 -10 eV above. This result is in good agreement with a previous calculation [7]. These features are observed in the XANES of LaB_6 single crystals. For a closer examination, we have plotted the experimental XANES (after oxide subtraction) together with the theoretical XANES (Wien k2 code) in Fig. 6.

From Fig. 6, we can see that the calculated XANES is in good agreement with experiment for both LaB_6 crystal and PLD film in the first 10 eV above the edge. The 187.36 eV energy position marks the Fermi level (binding energy) and the observed features at 188.76 eV, 189.79 eV and 192.73 eV are all reproduced albeit slightly shifted in energy. These features track the B p-DOS shown in Fig.5. Of particular interest is the onset of the threshold which is free electron-like indicating that the material is metallic. The sharp peak at 194.0 eV observed in the raw XANES data is not reproduced by theory supporting the notion that this peak is not originated from LaB_6 but from surface oxide. The sharp peak at 194.0 eV and the broad resonance at 201.9 eV in the TEY XANES of PLD LaB_6 film are characteristic of the π^* and σ^* of trigonal BO_3 structure, respectively in boron oxide, boric acid, or borates [18].

Returning to the XANES of the LaB_6 single crystal, we see that the features from 195 – 205 eV calculated by theory are only in qualitative agreement with experiment. The agreement improves if the final state lifetime broadening is included in the simulation [19]. Thus it is reasonable to conclude that B K-edge XANES of LaB_6 tracks the unoccupied p-DOS above the Fermi level, in semi-quantitative agreement with theory.

The XANES of the PLD LaB_6 film is very interesting in that it exhibits both sharp and broad features indicating that there is some disorder. From Fig. 6, we see that the XANES features of the PLD film within the first 5 eV above the threshold is nearly the same as those for the single crystal. This indicates that the LaB_6 signatures remain in the polycrystalline film of nanocrystallites (Fig. 2). The feature at 191.73 eV corresponds to the maximum of the p-DOS within the first 5 eV above the Fermi level. The much broader features suggest the lack of long range order. The most significant difference is found in the region of 5 – 15 eV above the threshold where the well-defined peaks at 198.61eV and 201.44 eV observed for the single crystal are broadened and shifted noticeably for the film. If we consider these two peaks for the LaB_6 single crystal as multiple scattering (shape resonance) peaks arising from the nearest and second nearest neighboring B atom of the absorbing atom, we may use the following phenomenological relation, which relates the shape resonance position to the bond lengths [20]

$$\Delta E = (E_{\sigma^*} - E_o) \propto \frac{1}{r} \qquad (1),$$

where E_{σ^*} is the energy position of the σ^* resonance and E_o is the crystal zero potential (e.g. muffin tin potential) and can be approximated with the threshold energy; r is the inter-atomic distance between the absorbing atom and the backscattering atom forming a covalent bond. This expression is valid, at least qualitatively, since $\sqrt{\Delta E} \propto k$, the wave vector, and k is inversely proportional to r, implying that the closer the energy position of the resonance to the threshold, the longer the bond. The proportionality varies however from the XANES region where multiple scattering dominates to the EXAFS region where single scattering dominates. We can attribute the 198.615 eV and the 201.42 eV resonances to the first and second nearest neighboring B atoms in the 6 B atom octahedron. If we let E_o = 187.46 eV, we get a second nearest neighbor distance to first nearest neighbor distance ratio, r_2/r_1 of 1.25 in qualitative agreement with the expected value of 1.41. Based on this analysis, we can infer that there is possible distortion to the B octahedron unit on the surface of the film and the nano grains since the 198.61 eV peak is shifted to slightly lower energy (~ 198 eV), corresponding to a slightly longer bond. The 202.0 eV peak is likely shifted slightly to higher energy but cannot be unambiguously identified due to broadening or residue contribution from surface impurities, such as oxygen which may also contribute to the distortion.

We now turn to identifying the surface/grain boundary structure of the PLD LaB_6 film as shown in the TEY XANES (Fig. 3c). We recall that we observed a very sharp resonance at 194.0 eV (π^* due to sp^2 bonding) and a very broad resonance (σ^*) at ~202 eV characteristic of a 3-coordinated B structure [18]. We ask what happens when the LaB_6 surface is exposed to the ambient. One possibility is the formation of a borate BO_3^{3-} structure, e.g. $LaBO_3$, another possibility is the formation of oxide such as B_2O_3. We also ask whether or not B in the B_6 unit in LaB_6 may be replaced with O atom when the unit is exposed to the surface (grain boundary). We explore the possibilities by conducting XANES simulations of the B K-edge XANES using FEFF8. Fig. 7 shows the simulation of the B K-edge XANES for $LaBO_3$ where the local structure of B is trigonal and B is coplanar with three oxygen atoms, and B_2O_3 where B is in a distorted tetrahedral environment. We see that the calculated $LaBO_3$ XANES clearly exhibits a sharp π^* type resonance and a broad σ^* type resonance and is in qualitative agreement with the XANES of the LaB_6 film recorded in TEY, which is dominated by surface contribution. The simulated B_2O_3 XANES, however exhibits similar features but at different energies. The experimental XANES for B_2O_3 is shown in the inset of Fig.7, which bears considerable

resemblance with the surface oxide of LaB_6. It is not entirely clear why FEEF can not reproduce these bound to bound transition features satisfactorily. Replacing B with C,N,O in the B_6 framework did not produce dramatic changes in the simulated XANES (not shown).

V Conclusion

The XANES result at the B K-edge of LaB_6 single crystal and Pulse Laser Deposited (PLD) films provides insights for the electronic structure of LaB_6 from the B perspective. It is founds that LaB_6 is metallic with primarily B sp character (B6 unit) in the conduction band, although the B-B interaction has considerable covalent character, that PLD LaB_6 film is largely polycrystalline with nanocrystals and the electronic structure in the vicinity of the Fermi level is essentially the same as single crystals, preserving the properties of bulk LaB_6 but providing a larger surface area; this explains why thermionic emission is enhanced in these films. Simulated XANES for LaB_6 single crystal using Density Functional Theory (DFT) is in reasonable agreement with experiment, especially in the first 5 eV region above the threshold. The surface of both LaB_6 single crystals and PLD films, especially the latter which has a large grain boundary, contains oxides. FEFF simulation produces less than satisfactory results and awaits further investigations.

Research at the University of Western Ontario is supported by NSERC, CRC, CFI and OIT. The Canadian Light Source is supported by CFI, NSERC, NRC, CIHR and the University of Saskatchewan. We thank Mark Beisinger of Surface Science Western for making the XPS measurements.

References

1. T. Lundstrom, Pure & Appl. Chem., ***57***, 1383 (1985).
2. N. A. Rae, Acta Cryst. ***A64***, C180 (2008).
3. H.M. Rietveld, J. Appl. Crystallography ***2***, 64 (1969)
4. D. P. Young, D. Hall, M. E. Torelli, Z. Fisk, J. L. Sarrao,J. D. Thompson, H.-R. Ott, S. B. Oseroff, R. G. Goodrichk R. Zysler, Nature, ***397***, 412 (1999).
5. J.J. Jia, J.H. Underwood, E.M. Gullikson, T.A. Callcott, and R.C.C. Perera, J. Electron Spectros. and Related Phenom. ***80,*** 509 (1996)
6. J.D. Denlinger, G.-H. Gweon, J.W. Allen, A.D. Bianchi, Z. Fisk, arXiv:cond-mat/0107426v1
7. F.M. Hossain, D.P. Riley and G.E. Murch, Phys. Rev. B, 72 235101 (2005)
8. P. Hohenberg and W. Kohn, Phys. Rev. **136**, B864 (1964); W. Kohn and L. J. Sham, Phys. Rev. A **140**, 1133 (1965).
9. J. P. Perdew and Y. Wang, Phys. Rev. B **45**, 13244 (1992).
10. P. Blaha and K. Schwarz, J. Phys. F ***17***, 899 (1987); P. Blaha, K. Schwarz, and P. Sorantin, and S. B. Trickey, Computer Phys. Comm., ***59***, 399 (1990).
11. A. L. Ankudinov, B. Ravel, J. J. Rehr, and S. D. Conradson, Phys. Rev. B ***58***, 7565 (1998).
12. X-ray calculator, CXRO website: http://henke.lbl.gov/optical_constants/
13. M. Kasrai, W.N. Lennard, R.W. Brunner, G.M. Bancroft, J.A. Bardwell and K.H. Tan, Appl. Surf. Sci. ***99***, 303 (1996).
14. T.K. Sham, Int. J. Nanotechnol., ***5***, 1194 (2008).
15. S.J. Mroczkowski, J. Vac. Sci. Technol. A***9*** 586 (1991).
16. S. Boughaba, G. I. Sproule, J. P. McCaffrey, M. Islam and M. J. Graham, Thin Soild Films, ***358***, 104 (2000).
17. Hu, Y.F.; L. Zuin, G. Wright, R. Igarashi, M. McKibben, T. Wilson, S.Y. Chen, T. Johnson, D. Maxwell, B.W. Yates, T.K. Sham, R. Reininger, Review of Scientific Instru. ***78***, 083109 (2007)
18. D. Xu and D. Peak, Environmental Science & Technology, ***41(3)*** 903 (2007)
19. J. E. Müller, O. Jepsen, J. W. Wilkins Solid State Communications, ***42***,365(1982).
20. M. Kasrai, M.E. Fleet, T.K. Sham, G.M. Bancroft, K.H. Tan and J.R. Brown, Solid Stat. Comm.***68***, 507-511 (1988).

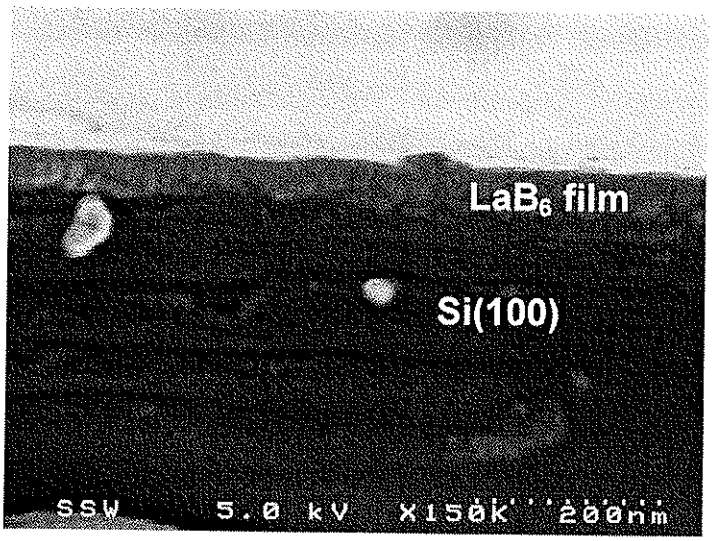

Figure 1: The cross-sectional FE-SEM micrographs of LaB_6 film deposited by PLD in vacuum at substrate temperatures of 300 °C

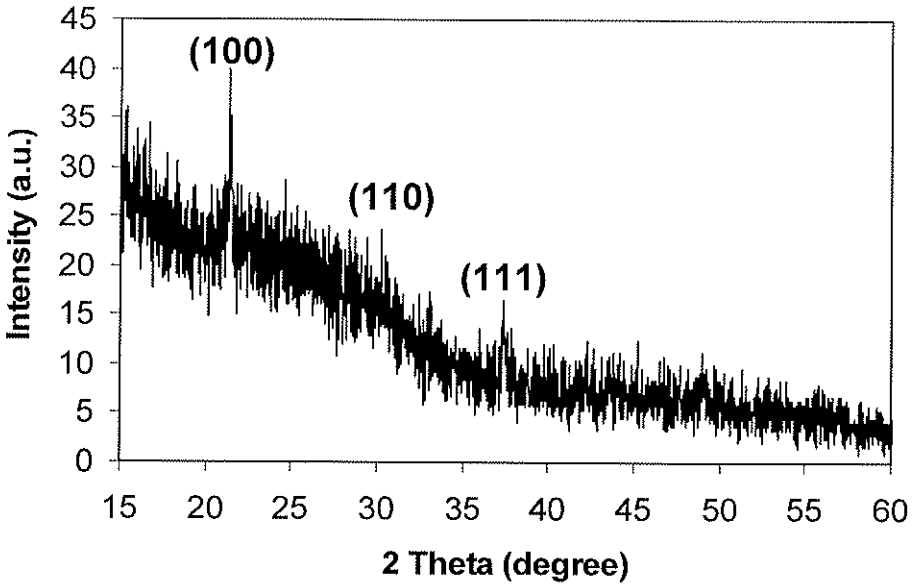

Figure 2: XRD pattern of LaB_6 film deposited by PLD in vacuum at substrate temperatures of 300 °C.

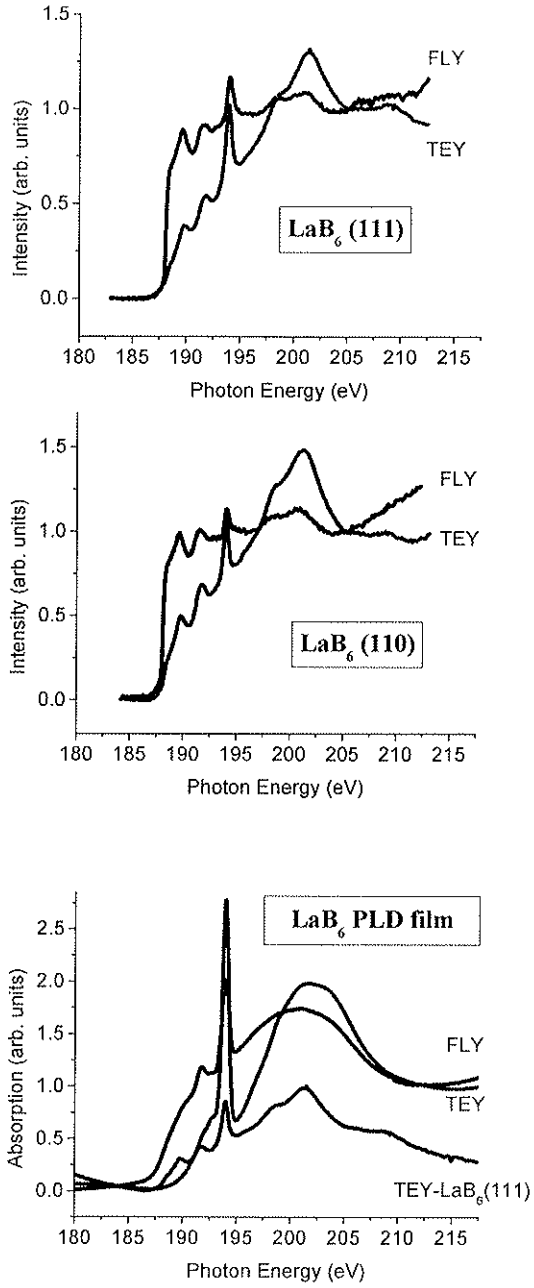

Figure 3. (a) TEY and FLY XANES of LaB_6: (a) LaB_6 (111), (b) LaB_6 (110) and (c) LaB_6 PLD film on Si (100). In (c), the LaB_6 (111) TEY XANES is also shown.

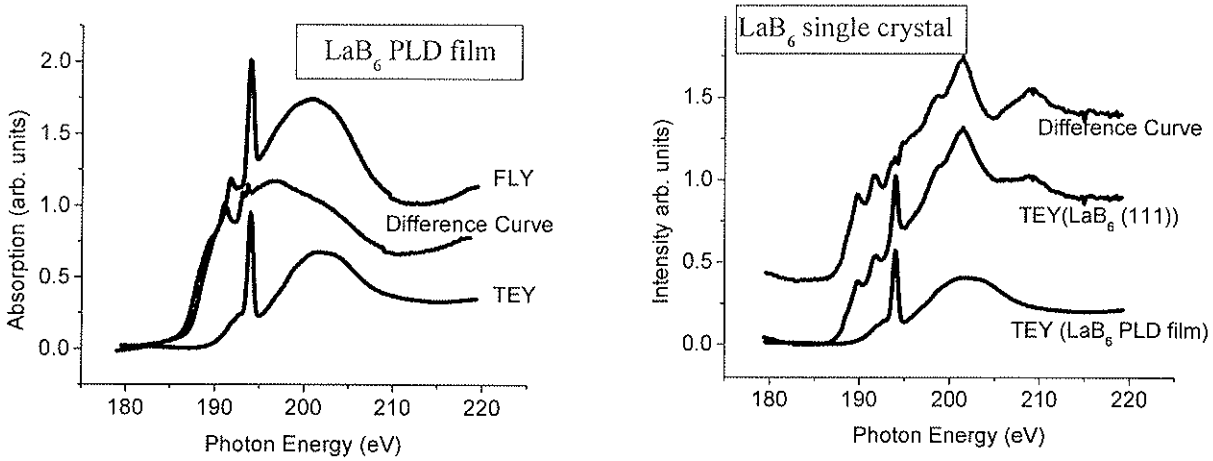

Figure 4. B K-edge XANES after the removal of surface oxide contributions: (a) LaB_6 PLD film on Si(100); (b) LaB_6 (111). The TEY of the film was scaled (as shown) and used to represent surface oxide contribution. The difference curve represents the XANES of the specimen with surface contribution minimized.

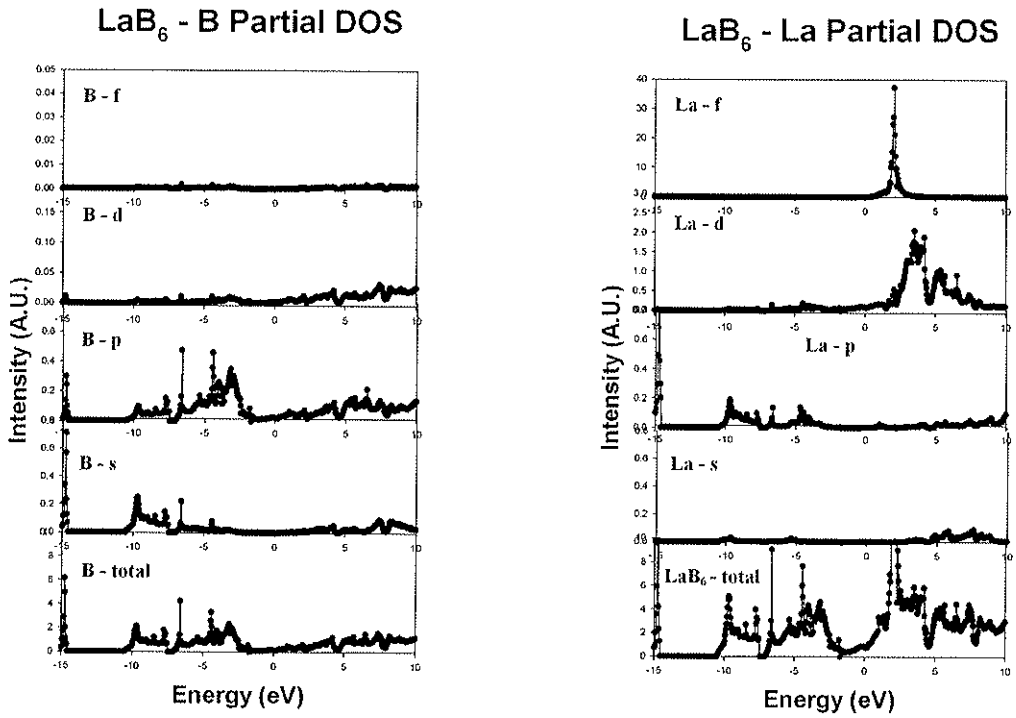

Figure 5. Theoretical partial densities of states (p –DOS) of B and La in LaB_6

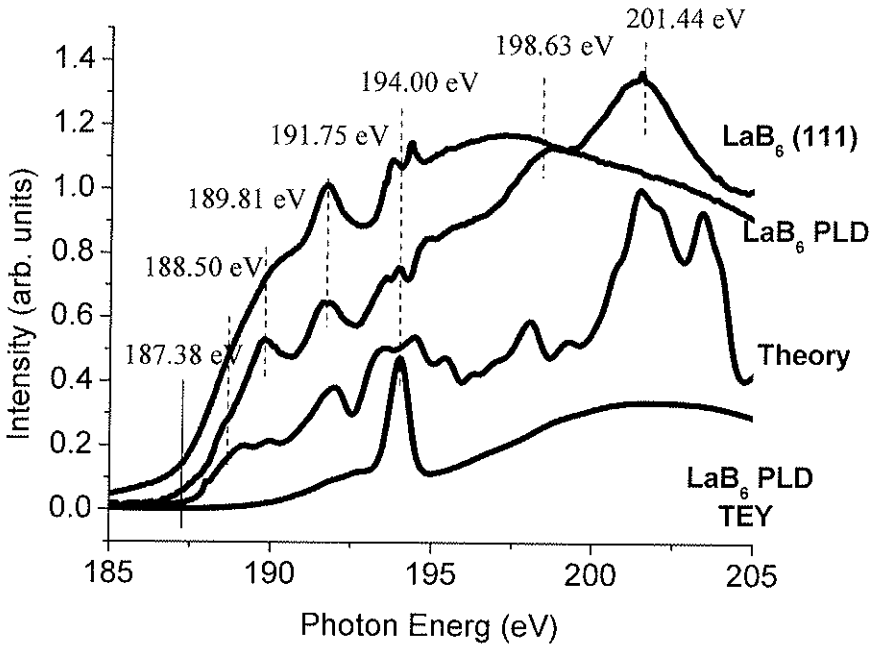

Figure 6 Comparison of LaB_6 XANES with theory; the LaB_6 PLD TEY is also display to show the position of the B oxide peak at 194.00 eV; The theoretical XANES were convoluted with core hole lifetime energy broadening as noted in the text and the energy positions of all the resonances are marked with a vertical line. The peak at 187.38 eV corresponds to the Fermi level.

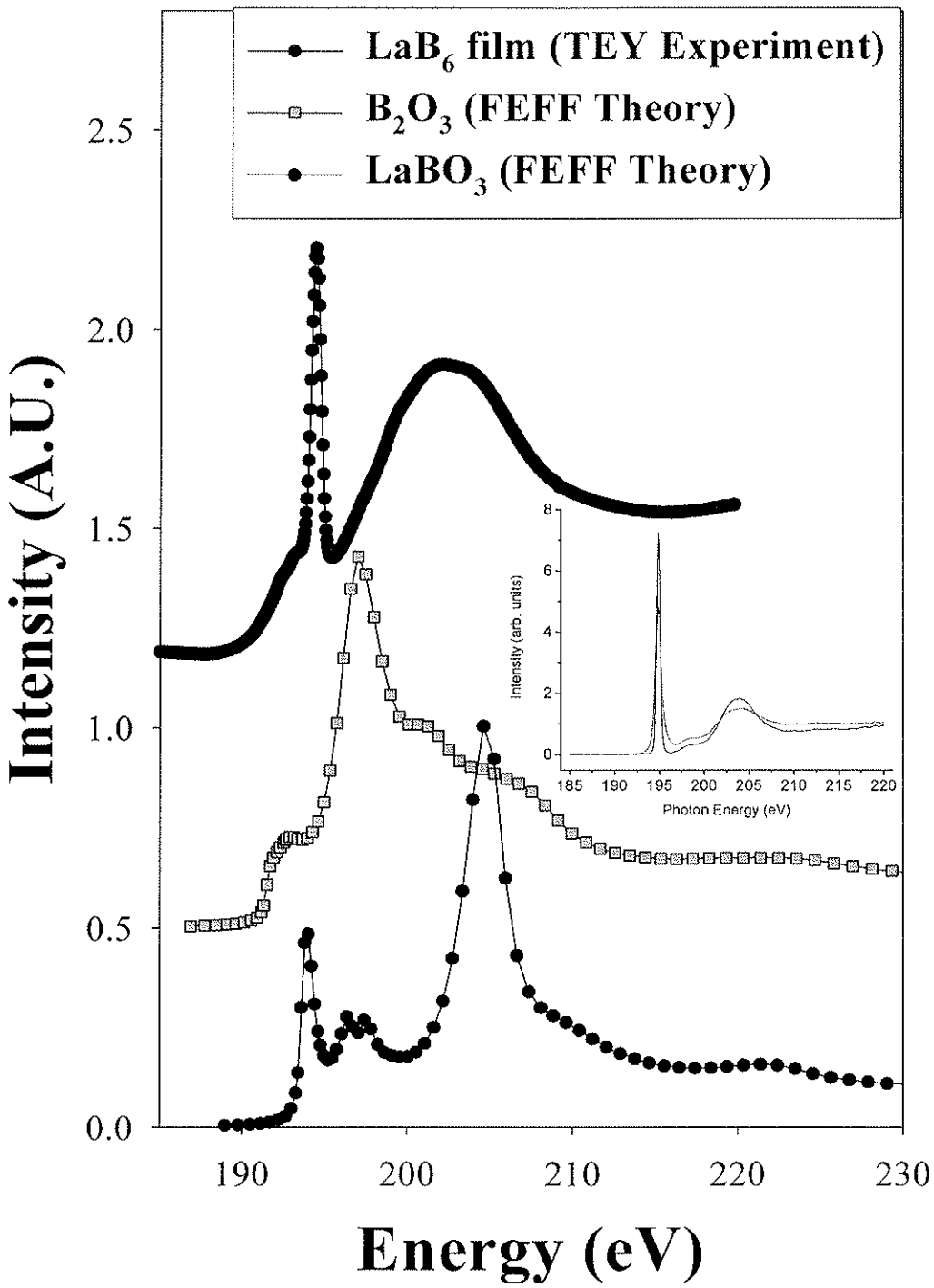

Figure 7 FEFF simulated XANES for B_2O_3 and $LaBO_3$, the XANES of LaB_6 PLD film recoded in TEY is also shown. The experimental XANES of B_2O_3 (TEY and FLY) are shown in the inset where the FLY resonances are slightly broader due to thickness effect.